

# An Improved Non-Iterative Surface Layer Flux Scheme for Atmospheric Stable Stratification Condition

Y. Li<sup>1,2</sup>, Z. Gao<sup>1,2</sup>, D. Li<sup>3</sup>, L. Wang<sup>2</sup>, and H. Wang<sup>1</sup>

[1]{Jiangsu Key Laboratory of Agriculture Meteorology, Collaborative Innovation Center on Forecast and Evaluation of Meteorological Disasters, College of Applied Meteorology, Nanjing University of Information Science and Technology, Nanjing, Jiangsu, China }

[2]{State Key Laboratory of Atmospheric Boundary Layer Physics and Atmospheric Chemistry, Institute of Atmospheric Physics, Chinese Academy of Sciences, Beijing, China }

[3]{Program of Atmospheric and Oceanic Sciences, Princeton University, Princeton, NJ 08540, USA }

Correspondence to: Z. Gao (zgao@mail.iap.ac.cn)

## Abstract

Parameterization of turbulent fluxes under stably stratified conditions has always been a challenge. Current surface fluxes calculation schemes either need iterations or suffer low accuracy. In this paper, a non-iteration scheme is proposed to approach the classic iterative computation results using multiple regressions. It can be applied to the full range of roughness status  $10 \leq z / z_0 \leq 10^5$  and  $-0.5 \leq \log(z_0 / z_{0h}) \leq 30$  under stable conditions  $0 < Ri_B \leq 2.5$ . The maximum (average) relative errors for the turbulent transfer coefficients for momentum and sensible heat are 12% (1%) and 9% (1%), respectively.

## 1 Introduction

In weather or climate models, earth surface is the boundary that needs to be resolved physically (Chen and Dudhia, 2001). The condition of atmosphere aloft (e.g., wind, temperature and humidity) is highly dependent on the momentum, sensible heat and latent heat fluxes at surface. Currently, the exchanges of momentum and heat between the earth surface and the atmosphere are usually calculated with various schemes based on Monin-Obukhov similarity theory (hereinafter MOST, Monin and Obukhov, 1954) in models. These schemes (e.g., Paulson, 1970;

1 Businger, 1971; Dyer 1974; Holtslag and De Bruin, 1988, Beljaars and Holtslag, 1991; Janjić  
2 1994; Launiainen, 1995; Högström, 1996) are similar to each other but the differences among  
3 them exist due to different observational data and/or mathematical solutions that were used in  
4 retrieving the schemes. One commonly used scheme is Businger-Dyer (BD) equation (Businger,  
5 1966; Dyer, 1967). However, the BD equation suppresses fluxes under stable condition too  
6 quickly and is not applicable when the Richardson number exceeds a critical value (Louis,  
7 1979). Holtslag and De Bruin (1988) and Beljaars and Holtslag (1991) proposed alternative  
8 schemes which can be used under very stable conditions. With data collected in the field  
9 program CASES-99 (Cooperative Atmosphere-Surface Exchange Study-99) (Poulos et al.,  
10 2002), Cheng and Brutsaert (2005, CB05 hereinafter) further provided a new scheme and it is  
11 confirmed to perform better by later research (Guo and Zhang, 2007; Jiménez et al, 2012).  
12 Based on the measurements made during experiment SHEBA in Arctic and Halley 2003  
13 experiment in Antarctica, Grachev et al. (2007) and Sanz Rodrigo and Anderson (2013)  
14 proposed different similarity functions, respectively. Through systematic mathematical analysis,  
15 Sharan and Kumar (2011) proved that similarity functions of CB05 and Grachev et al. (2007)  
16 were applicable in the whole stable stratification region. However, all of these studies are based  
17 on MOST and application of MOST in very stable condition is in doubt since it assumes that  
18 turbulence is continuous and stationary, while in very stable condition turbulence is weak,  
19 sporadic and patchy (Sharan and Kumar, 2011). Grachev et al. (2013) indicates that the  
20 applicability of local MOST in stable conditions is limited by the inequalities, when both  
21 gradient and flux Richardson numbers are below their "critical values" about 0.20-0.25. Further,  
22 MOST predicts that mean gradients of turbulence become independent of z in very stable  
23 condition, Wyngaard and Coté (1972) first referred to this limit as 'z-less stratification'. BD  
24 equations follow this prediction, but CB05 and Grachev et al. (2007) do not. To avoid these  
25 holdbacks and self-correlation of MOST, Sorbjan (2010) and Sorbjan and Grachev (2010)  
26 discussed an alternative local scaling for the stable boundary layer (referred to as gradient-based  
27 scaling) when different universal functions plotted versus the gradient Richardson number  
28 instead of the Monin-Obukhov stability parameter.

29 Another critical issue regarding the fluxes calculation with MOST is the numerical iteration.  
30 Under unstable condition, the iteration normally converges within 5 steps (Fairall et al, 1996).  
31 By taking advantage of a bulk Richardson number parameterization for an improved first guess  
32 (Grachev and Fairall, 1997), the iteration can be reduced to 3 steps (Fairall et al, 2003). In the  
33 Weather Research Forecasting (WRF) model (Skamarock et al., 2008) MM5 similarity surface

1 **module**, the flux variables from the previous time step are used to calculate the fluxes at current  
2 time step and such an approach can yield reasonable result (Jiménez et al, 2012). On the other  
3 hand, under stable condition, the flux calculation takes many more steps to converge and hence  
4 is time consuming. To avoid the iteration process, a series of non-iterative schemes are proposed  
5 (e.g., Loius, 1979, Garratt, 1992, Launiainen, 1995, Song, 1998, De Bruinet al. 2000, Yang et  
6 al., 2001; Li et al., 2010), but they all fail to cover the full range of  $-0.5 \leq kB^{-1} \leq 30$  ,  
7  $10 \leq z/z_0 \leq 10^5$  and  $-5.0 \leq Ri_B \leq 2.5$ , which is pointed out by Wouters et al. (2012, WRL12  
8 hereinafter). Here  $kB^{-1} = \ln(z_0/z_{0h})$  .  $z$  is the reference height; and  $z_0$  and  $z_{0h}$  are the  
9 aerodynamic and thermal roughness lengths, respectively.  $Ri_B$  is the bulk Richardson number.  
10 **Following WRL12, the condition that  $Ri_B > 2.5$  is not considered in this study, because it**  
11 **represents extremely stable stratification with very weak wind and little flux exchange.** To  
12 calculate fluxes under all conditions, and also to include the roughness sublayer effect, WRL12  
13 proposed an updated scheme **based on the iterated results of CB05 under stable condition.**  
14 However, for a given  $Ri_B$ , WRL12 uses only one equation to cover the whole large range of  
15  $z/z_0$  and  $kB^{-1}$ , which results in biases at some  $z/z_0$  and  $kB^{-1}$  conditions. Therefore, to avoid  
16 the iteration process and keep the accuracy at the same time, **the objective of this paper is to**  
17 **propose** a group of equations that divide the calculation into 8 regions according to  $z_0$  and  $z_{0h}$   
18 values. **To compare with WRL12, and with the fact that CB05 equations are currently widely**  
19 **accepted, the new equations are also based on the iterated results of CB05 equations.** Section 2  
20 describes the calculation results from CB05 and WRL12. Section 3 introduces the new  
21 equations, and section 4 intercompares these schemes. Summary and conclusions are presented  
22 in section 5

## 23 **2 Revisiting CB05 and WRL12**

24 The momentum flux  $\tau$  and sensible heat flux  $H$  are defined as:

$$25 \quad \tau \equiv \rho u_*^2 \quad (1)$$

$$26 \quad H \equiv -\rho c_p u_* \theta_* \quad (2)$$

27 Here  $u_*$  is the friction velocity,  $\theta_*$  is the temperature scale,  $\rho$  the air density and  $c_p$  the  
28 specific heat capacity at constant pressure. Based on MOST, the friction velocity  $u_*$  and  
29 temperature scale  $\theta_*$  can be calculated by:

$$1 \quad u_* = uk / [\ln(\frac{z}{z_0}) - \psi_m(\frac{z}{L}) + \psi_m(\frac{z_0}{L}) + \psi_m^*(\frac{z}{L}, \frac{z}{z_*})] \quad (3)$$

$$2 \quad \theta_* = (\theta - \theta_0)k / [\ln(\frac{z}{z_{0h}}) - \psi_h(\frac{z}{L}) + \psi_h(\frac{z_{0h}}{L}) + \psi_h^*(\frac{z}{L}, \frac{z}{z_*})] \quad (4)$$

3 Here  $u$  and  $\theta$  are the wind speed and potential temperature at the reference height  $z$ .  $k$  is the  
4 von Karman constant.  $z_*$  is the roughness sublayer height.  $\theta_0$  is the potential temperature at the  
5 height of  $z_{0h}$ .  $\psi_m$  and  $\psi_h$  are the integrated stability functions for momentum and heat,  
6 respectively.  $\psi_m^*$  and  $\psi_h^*$  are the correction functions account for roughness sublayer effect.  $L$   
7 is the Obukhov length defined as:

$$8 \quad L \equiv u_*^2 \bar{\theta} / (kg\theta_*) \quad (5)$$

9  $\psi_m^*$  and  $\psi_h^*$  are given by De Ridder (2010):

$$10 \quad \psi_{m,h}^*(\frac{z}{L}, \frac{z}{z_*}) = \int_z^\infty \frac{\phi_{m,h}(\frac{z'}{L})}{z'} e^{-\mu_{m,h} \frac{z'}{z_*}} dz' \quad (6)$$

11  $\mu_m = 2.59$ ,  $\mu_h = 0.95$ , and  $\phi_{m,h}$  are the stability functions for momentum and heat. Following  
12 Sarkar and De Ridder (2010) and WRL12,  $z_*/z_0 = 16.7$  is adopted in this study.

13 CB05 gives the form of  $\phi_{m,h}$  and  $\psi_{m,h}$ :

$$14 \quad \phi_m = 1 + a \frac{\zeta + \zeta^b (1 + \zeta^b)^{\frac{1-b}{b}}}{\zeta + (1 + \zeta^b)^{\frac{1}{b}}} \quad (7)$$

$$15 \quad \phi_h = 1 + c \frac{\zeta + \zeta^d (1 + \zeta^d)^{\frac{1-d}{d}}}{\zeta + (1 + \zeta^d)^{\frac{1}{d}}} \quad (8)$$

$$16 \quad \psi_m = -a \ln(\zeta + (1 + \zeta^b)^{\frac{1}{b}}) \quad (9)$$

$$17 \quad \psi_h = -c \ln(\zeta + (1 + \zeta^d)^{\frac{1}{d}}) \quad (10)$$

18 Here  $a = 6.1$ ,  $b = 2.5$ ,  $c = 5.3$  and  $d = 1.1$ .  $\zeta \equiv z/L$  is the stability parameter.

1 With Eqs. (3), (4), (5), and (6),  $\phi_{m,h}$  and  $\psi_{m,h}$  of CB05, fluxes can be calculated through  
2 iterations: with a first guess of  $\zeta$ ,  $u_*$  and  $\theta_*$  can be calculated from Eqs. (3) and (4), then  $\zeta$   
3 again can be derived from Eq. (5). This procedure iterates until the results converge. The  
4 relationships of  $\zeta \sim Ri_B$ ,  $\zeta \sim \ln(z/z_0)$ , and  $\zeta \sim \ln(z_0/z_{0h})$  from CB05 are shown in Fig. 1, Fig. 2  
5 and Fig. 3, respectively. **Conditions with  $Ri_B = 0.05, 0.2, 0.5$ ,  $z/z_0 = 10, 1000, 10^5$  and**  
6  **$kB^{-1} = -0.5, 15, 30$  are plotted.** However, due to the limitation of computational time in  
7 numerical weather and climate models, the calculation results after 5 steps are always taken to  
8 approximate the fluxes (e.g., MYJ and MYNN surface module in WRF model, Janjić, 1996,  
9 Nakanishi M, Niino, 2006). It is found that with the first guess of  $\zeta_0 = Ri_B \frac{[\ln(z/z_0)]^2}{\ln(z/z_{0h})}$  and 5  
10 steps of iteration, the results are still far away from the precise value. **Fig. 4 presents the relative**  
11 **error  $\Delta\zeta$  for various  $Ri_B$  with  $z/z_0 = 10, 1000, 10^5$  and  $kB^{-1} = -0.5, 15, 30$ .** The relative error  
12  $\Delta\zeta$  that is calculated by Eq. 11 can exceed 70% under certain conditions.

$$13 \quad \Delta\zeta = \begin{cases} \frac{|\zeta_{(cal)} - \zeta_{(precise)}|}{\zeta_{(precise)}} \times 100\%, & \text{for } |\zeta_{(cal)} - \zeta_{(precise)}| \geq 0.01 \\ 0, & \text{for } |\zeta_{(cal)} - \zeta_{(precise)}| < 0.01 \end{cases} \quad (11)$$

14 where  $\zeta_{(cal)}$  is the calculation result, and  $\zeta_{(precise)}$  is the precise result from the ultimate iteration  
15 of CB05 (when  $|\zeta_{(n+1)} - \zeta_{(n)}| < 0.1\% \zeta_{(n)}$ ,  $\zeta_{(n)}$  is adopted as  $\zeta_{(precise)}$ , and here n indicates the  
16 iteration step). **Fig. 5 shows the steps needed to converge into 5% relative error with CB05**  
17 **equations for various  $Ri_B$  with  $z/z_0 = 10, 1000, 10^5$  and  $kB^{-1} = -0.5, 15, 30$ . It shows that when**  
18  **$Ri_B = 0.74$ ,  $z/z_0 = 10$  and  $kB^{-1} = 30$ ,** more than 80 steps of iteration are needed to reduce the  
19 calculation error within 5%. The iteration takes more steps to converge when there is a larger  
20 aerodynamic roughness length  $z_0$  and a smaller thermal roughness length  $z_{0h}$ , which is  
21 common over an urban surface (Sugawara and Narita, 2009). When  $z/z_0 = 10$  and  $kB^{-1} = 30$ ,  
22 the largest error can reach 75% after 5 steps iteration (Fig. 4) and 82 steps are needed for the  
23 results to converge (Fig. 5). However, when  $z/z_0$  becomes large, for example  $z/z_0 = 10^5$  (i.e.,  
24 a representative value for a smooth sea surface), 5 steps are enough for the results to be within  
25 5% error under all  $kB^{-1}$  and  $Ri_B$  conditions (Fig. 5).

1 To avoid the iteration, and based on CB05's iteration results, WRL12 proposed the following  
 2 set of equations:

$$3 \quad \zeta_t = -0.316 - 0.515e^{-L_{0H}} + 25.8e^{-2L_{0H}} + 4.36L_{0H}^{-1} - 6.39L_{0H}^{-2}, \quad (12)$$

$$+ 0.834 \log(L_{0M}) - 0.0267 \log^2(L_{0M})$$

$$4 \quad Ri_{B,t} = \zeta_t \frac{L_{0H}^* + S_{0H}^* \beta_H \zeta_t}{(L_{0M}^* + S_{0M}^* \beta_M \zeta_t)^2}, \quad (13)$$

$$5 \quad \zeta = \frac{-L_{0M}^*}{S_{0M}^* \beta_M} - \frac{BC}{4(S_{0M}^* \beta_M)^3 (B^2 + |Cr|)} + \frac{B - \sqrt{B^2 + Cr} + \frac{BCr}{2(B^2 + |Cr|)}}{2(S_{0M}^* \beta_M)^3 r}, \quad (\text{for } Ri_B \leq Ri_{B,t}), \quad (14)$$

$$6 \quad \zeta = \zeta_t + D(\zeta_t)(Ri_B - Ri_{B,t}), \quad (\text{for } Ri_B > Ri_{B,t}), \quad (15)$$

$$7 \quad D(\zeta_t) = \frac{(L_{0M}^* + S_{0M}^* \beta_M \zeta_t)^3}{L_{0M}^* L_{0H}^* + \zeta_t (2S_{0H}^* \beta_H L_{0M}^* - S_{0M}^* \beta_M L_{0H}^*)}, \quad (16)$$

8 where

$$9 \quad L_{0i} = \ln(z / z_{0i}), \quad (i \text{ stands for M or H}), \quad (17)$$

$$10 \quad L_{0i}^* = L_{0i} + \frac{1}{\lambda} \ln\left(1 + \frac{\lambda}{\mu_i \frac{z}{z_*}}\right) e^{-\mu_i \frac{z}{z_*}}, \quad (i \text{ stands for M or H}), \quad (18)$$

$$11 \quad r = Ri_B - S_{0H}^* \beta_H / (S_{0M}^* \beta_M)^2 \quad (19)$$

$$12 \quad B = S_{0M}^* \beta_M L_{0H}^* - 2S_{0H}^* \beta_H L_{0M}^* \quad (20)$$

$$13 \quad C = 4(S_{0M}^* \beta_M)^2 L_{0M}^* (S_{0H}^* \beta_H L_{0M}^* - S_{0M}^* \beta_M L_{0H}^*) \quad (21)$$

$$14 \quad S_{0i}^* = 1 - z_{0i} / z + \left(1 + \frac{\nu}{\mu_i \frac{z}{z_*}}\right) \frac{1}{\lambda} \ln\left(1 + \frac{\lambda}{\mu_i \frac{z}{z_*}}\right) e^{-\mu_i \frac{z}{z_*}} \quad (22)$$

15 where  $\lambda = 1.5$ ,  $\nu = 0.5$ ,  $\beta_M = 4.76 + 7.03z_0 / z + 0.24z_{0h} / z_0$  and  $\beta_H = 5$ . First,  $Ri_{B,t}$  is calculated  
 16 from Eqs. (12) and (13), and then  $\zeta$  can be derived from Eqs. (14) or (15). **Fig. 6 presents the**  
 17 **relative error of  $\zeta$  with WRL12 equations compared with iterated results of CB05 for various**

1  $Ri_B$  with  $z/z_0 = 10, 1000, 10^5$  and  $kB^{-1} = -0.5, 15, 30$ . It shows that the relative error of WRL12  
 2 exceeds 20% when  $Ri_B$  is small, and exceeds 50% when  $Ri_B$  becomes large.

### 3 Derivation of the new scheme

4 It can be seen from Fig. 1, Fig. 2 and Fig. 3 that  $\zeta$  varies with  $Ri_B$ ,  $\log(z/z_0)$  and  $kB^{-1}$  with  
 5 remarkable nonlinearity. Specially, when  $kB^{-1}$  is large,  $\zeta \sim z_0$  relationship can hardly be  
 6 approximated by a cubic equation at some  $Ri_B$  values (Fig. 2). Correspondingly, when  $z_0$  is  
 7 large,  $\zeta \sim z_{0h}$  also needs a high power series equation to approximate (at least cubic fit is not  
 8 enough, Fig. 3). Therefore, similar to the division of  $Ri_B$  into weakly and strongly stable  
 9 conditions in order to reduce the complexity of regression (e.g., Lauriainen, 1991; Li et al.,  
 10 2010; WRL12), in this paper, multiple regions are divided with  $z_0$  and  $z_{0h}$  values and  
 11 regressions of  $\zeta = f(Ri_B, L_{0M}, kB^{-1})$  are conducted in these regions. In this way, the complexity  
 12 of the equations can be reduced and at the same time their accuracy can be maintained. Although  
 13 the total number of equations is increased due to the division of  $z_0$  and  $z_{0h}$ , the calculation  
 14 efficiency is still enhanced since the logical judgment of the region according to  $z_0$  and  $z_{0h}$   
 15 values in programme codes takes much less time than iterations. The critical issue here is how  
 16 to divide the  $z_0$  and  $z_{0h}$  regions in a reasonable way to obtain the smallest number of regions  
 17 but the highest accuracy. For this purpose, the  $z_0$  and  $z_{0h}$  are first divided into 13 and 14  
 18 sections according to the values of  $z/z_0$  and  $z_0/z_{0h}$ , respectively. For  $z/z_0$ , the sections are  
 19 10~20, 20~40, 40~80, ..., 10240~20480, 20480~40960 and 40960~ $10^5$ ; for  $z_0/z_{0h}$ , the  
 20 sections are 0.607~1, 1~10, 10~100, 100~ $10^3$ ,  $10^3$ ~ $10^4$ , ...,  $10^{11}$ ~ $10^{12}$  and  $10^{12}$ ~ $1.07 \times 10^{13}$ .  
 21  $z/z_0 \in 10 \sim 20$  and  $z_0/z_{0h} \in 10^{12} \sim 1.07 \times 10^{13}$  is the region that needs the highest power  
 22 series equation to approximate. This region is firstly chosen to find a maximum critical value  
 23 of  $\zeta_{c1}$  that can make the regression:

$$24 \quad \zeta = f(Ri_B, L_{0M}, kB^{-1}) = Ri_B \sum C_{ijk} Ri_B^i L_{0M}^j (L_{0H} - L_{0M})^k \quad (23)$$

25 be within 5% error when  $\zeta \in 0 \sim \zeta_{c1}$ . Here  $i, j$ , and  $k = 0, 1, 2$ , and  $3$ , and  $i + j + k \leq 4$ .  $C_{ijk}$  are  
 26 the coefficients from regression. It is found that  $\zeta_{c1} = 0.33$  meets this criterion. Then some of

1 the  $z_0$  and  $z_{0h}$  regions can be merged with each other for the section  $\zeta \in 0 \sim 0.33$  and a total of  
 2 8  $z_0 - z_{0h}$  regions are left in the  $z_0 - z_{0h}$  plane. In other words, the regression error of Eq. (23)  
 3 can be kept within 5% in any of the 8 regions when  $\zeta \in 0 \sim 0.33$  (Table 1). Thus, for these 8  
 4 regions, it can be found that with the sections divided by the specified critical values  $\zeta_{cp}$  (where  
 5 p is 1,2,3, ... it indicates the section and its maximum value depends on the  $z_0 - z_{0h}$  region), the  
 6 regression error with Eq. (23) can be kept within 5% for  $\zeta \leq 0.5$  and 10% or  $\zeta > 0.5$ . For a  
 7 given pair of  $z_0$  and  $z_{0h}$ , the division by  $\zeta_{cp}$  can be transformed to  $Ri_{Bcp}$ :

$$8 \quad Ri_{Bcp} = \sum C_{mm} \log^m(L_{0M}) (L_{0H} - L_{0M})^n \quad (24)$$

9 Here m, n = 0, 1, 2, and  $m + n \leq 3$ ; p is 1,2,3, ..., which indicates the section and its maximum  
 10 value depends on the  $z_0 - z_{0h}$  region. For region 1 and 7, the maximum p is 6, while for other  
 11 regions it varies between 3 and 5. The coefficients for Eq. (24) are shown in Table 2. The  $Ri_{Bcp}$   
 12 then cut the 0-2.5  $Ri_B$  range into several sections: section 1 is from 0 to  $Ri_{Bc1}$ , section 2 from  
 13  $Ri_{Bc1}$  to  $Ri_{Bc2}$ , and so on. The coefficients for Eq. (23) in each section are given in Tables 3~10.

14 **The procedure to obtain these coefficients are summarized below:**

15 1) Divide  $z/z_0$  into 13 sections: 10~20, 20~40, 40~80, ..., 10240~20480, 20480~40960 and  
 16 40960~ $10^5$ ; divide  $z_0/z_{0h}$  in to 14 sections: 0.607~1, 1~10, 10~100, 100~ $10^3$ ,  $10^3 \sim 10^4$ , ..., ,  
 17  $10^{11} \sim 10^{12}$  and  $10^{12} \sim 1.07 \times 10^{13}$ .

18 2) Use the region  $z/z_0 \in 10 \sim 20$  and  $z_0/z_{0h} \in 10^{12} \sim 1.07 \times 10^{13}$  to find  $\zeta_{c1}$ .  
 19 Method: when  $\zeta \in 0 \sim \zeta_{c1}$ , regression with Eq. (23) is kept within 5% error.

20 Result:  $\zeta_{c1} = 0.33$  found.

21 3) Use  $\zeta_{c1} = 0.33$  to recombine  $z/z_0$  and  $z_0/z_{0h}$  sections defined in step 1.  
 22 Method: Variations of combinations of the 13 sections of  $z/z_0$  and 14 sections of  $z_0/z_{0h}$   
 23 are tested to minimize the numbers of regions, and regression with Eq. (23) and  
 24  $\zeta \in 0 \sim 0.33$  is kept within 5% error.

25 Result: 8 regions found (Table 1)

26 4) For each of the 8 regions, find  $\zeta_{c1}, \zeta_{c2}, \dots, \zeta_{cp}, \dots$

27 Method: when  $\zeta \in 0 \sim \zeta_{c1}$ , or  $\zeta_{c1} \sim \zeta_{c2}$ , ..., or  $\zeta_{c(p-1)} \sim \zeta_{cp}$ , ..., regression with Eq. (23) is



1 kept within 5% error for  $\zeta \leq 0.5$  and 10% error for  $\zeta > 0.5$ .

2 Result:  $\zeta_{c1}, \zeta_{c2}, \dots, \zeta_{cp}, \dots$ , for each region found

3 5) Transfer  $\zeta_{c1}, \zeta_{c2}, \dots, \zeta_{cp}, \dots$ , to  $Ri_{Bc1}, Ri_{Bc2}, \dots, Ri_{Bcp}, \dots$ , with Eq. (24)

4 Method: for each region, when  $Ri_B \in 0 \sim Ri_{Bc1}$ , or  $Ri_{Bc1} \sim Ri_{Bc2}, \dots$ , or

5  $Ri_{Bc(p-1)} \sim Ri_{Bcp}, \dots$ , regression with Eq. (23) is kept within 5% error for  $\zeta \leq 0.5$  and 10%  
6 error for  $\zeta > 0.5$ .

7 Result: coefficients of Eq. (23) and Eq. (24) are derived.

8 The calculation procedure for a given group of  $z_0, z_{0h}$  and  $Ri_B$  is that: 1) find the region  
9 according to  $z_0$  and  $z_{0h}$  with Table 1; 2) Find the section according to the region and  $Ri_B$  with  
10 Eq. (24) and coefficients in Table 2; and 3) In Table 3-10 find the coefficients for the particular  
11 region and section and use Eq. (23) to calculate  $\zeta$ . Fig. 7 presents the relative error of  $\zeta$  with  
12 new equations compared with iterated results of CB05 for various  $Ri_B$  with  $z/z_0 = 10, 1000, 10^5$   
13 and  $kB^{-1} = -0.5, 15, 30$ . With the new equations, the relative error is controlled to be within 10%  
14 for the whole range. Specially, when  $\zeta \leq 0.5$ , the relative error is within 5% since it happens  
15 more often in the real conditions (Fig. 8).

16

#### 17 4 Comparison of the results from CB05 with 5 steps iteration, WRL12 and the 18 new scheme

19 The maximum and average relative error of  $\zeta$ ,  $C_M$  and  $C_H$  calculated from CB05 with 5 steps  
20 iteration, WRL12 and the new scheme are shown in Fig. 8, Fig. 9 and Fig. 10 for various  $\zeta$   
21 with  $z/z_0 = 10, 1000, 10^5$  and  $kB^{-1} = -0.5, 15, 30$ .  $C_M$  and  $C_H$  are the transfer coefficients for  
22 momentum and sensible heat respectively, and:

$$23 \quad C_M = \frac{k^2}{\left[ \ln\left(\frac{z}{z_0}\right) - \psi_m(\zeta) + \psi_m\left(\frac{z_0}{z}\zeta\right) + \psi_m^*\left(\zeta, \frac{z}{z_*}\right) \right]^2} \quad (25)$$

$$24 \quad C_H = \frac{k^2}{\left[ \ln\left(\frac{z}{z_0}\right) - \psi_m(\zeta) + \psi_m\left(\frac{z_0}{z}\zeta\right) + \psi_m^*\left(\zeta, \frac{z}{z_*}\right) \right] \left[ \ln\left(\frac{z}{z_{0h}}\right) - \psi_h(\zeta) + \psi_h\left(\frac{z_0}{z}\zeta\right) + \psi_h^*\left(\zeta, \frac{z}{z_*}\right) \right]} \quad (26)$$

1 To speed up the calculation,  $\psi_{m,h}^*(\zeta, \frac{z}{z_*})$  here is not calculated from Eq. (6) but rather from the  
 2 non-integral equation proposed by De Ridder (2010):

$$3 \quad \psi_{m,h}^*(\zeta, \frac{z}{z_*}) = \phi_{m,h} \left[ \left(1 + \frac{\nu}{\mu z / z_*}\right) \zeta \right] \frac{1}{\lambda} \ln \left(1 + \frac{\lambda}{\mu z / z_*}\right) \exp(-\mu z / z_*) \quad (27)$$

4 Where  $\lambda = 1.5$ ,  $\mu = \mu_m = 2.59$ ,  $\mu = \mu_h = 0.95$  and  $\nu = 0.5$ . The relative error for  $C_M$  and  $C_H$  is  
 5 calculated from:

$$6 \quad \Delta C_{M,H} = \frac{|C_{M,H(\text{cal})} - C_{M,H(\text{precise})}|}{C_{M,H(\text{precise})}} \times 100\% \quad (28)$$

7 where  $C_{M,H(\text{cal})}$  is calculated with  $\zeta_{(\text{cal})}$  from the three different methods, and  $C_{M,H(\text{precise})}$  is  
 8 calculated with  $\zeta_{(\text{precise})}$  from the ultimate iteration of CB05.

9 Maximum error indicates the maximum error for a particular  $\zeta$  under various  $z_0$  and  $z_{0h}$   
 10 conditions, while average error is calculated from

$$11 \quad \text{AverageError}(\zeta) = \frac{\int_{-0.5 \log(10)}^{30 \log(10^5)} \int_{\frac{z_0}{z_*}}^{\frac{z_{0h}}{z_*}} \text{Error}(\zeta) d \log\left(\frac{z}{z_*}\right) d \log\left(\frac{z_0}{z_{0h}}\right)}{\int_{-0.5 \log(10)}^{30 \log(10^5)} \int_{\frac{z_0}{z_*}}^{\frac{z_{0h}}{z_*}} d \log\left(\frac{z}{z_*}\right) d \log\left(\frac{z_0}{z_{0h}}\right)} \quad (29)$$

12 Here  $\text{Error}(\zeta)$  indicates  $\Delta\zeta$  or  $\Delta C_{M,H}$  at a particular  $\zeta$ . Although Eq. (28) presents the form of  
 13 continuous integral, it is actually calculated discretely with interval 0.035 for  $\log(\frac{z}{z_*})$  and 0.1  
 14 for  $\log(\frac{z_0}{z_{0h}})$ .

15 The results indicate that the maximum  $\Delta\zeta$  can be significant (exceeds 50%) when using CB05  
 16 with 5 steps iteration or WRL12. Correspondingly, the average  $\Delta\zeta$  for the two methods both  
 17 exceeds 15%. While with the new scheme, the maximum  $\Delta\zeta$  is always smaller than 5% (when  
 18  $\zeta \leq 0.5$ ) and 10% (when  $\zeta > 0.5$ ), and the average  $\Delta\zeta$  is always smaller than 2% in the whole  
 19 range. The maximum  $\Delta C_M$  from CB05 with 5 steps iteration (WRL12) exceeds 50% (40%),  
 20 and average  $\Delta C_M$  exceeds 30% (8%). The maximum  $\Delta C_H$  from CB05 with 5 steps iteration

1 (WRL12) exceeds 50% (24%), and average  $\Delta C_H$  exceeds 18% (6%). Comparatively, the new  
2 scheme controls the maximum  $\Delta C_M$  ( $\Delta C_H$ ) to be within 12% (9%) and the average  $\Delta C_M$  ( $\Delta C_H$ )  
3 within 1% (1%).

## 4 **5 Summary and conclusions**

5 Although CB05 provides a way to calculate surface fluxes under stable condition, its practical  
6 usage is confined due to the involved iteration process. It has been shown that iteration with 5  
7 steps will result in large calculation errors, especially when  $z/z_0$  is small and  $kB^{-1}$  is large,  
8 which is common over an urban surface. WRL12 proposed a way to avoid the iteration, but its  
9 calculation accuracy can be improved. Through dividing the  $z_0 - z_{0h}$  plane into 8 regions, the  
10 new scheme develops a group of equations with higher accuracy. The calculation error of  
11  $\zeta = f(Ri_B, L_{0M}, kB^{-1})$  is always controlled to be within 5% (when  $\zeta \leq 0.5$ ) and 10% (when  
12  $\zeta > 0.5$ ). The calculation procedure is also simple, for a small  $Ri_B$  (i.e.,  $Ri_B < Ri_{Bc1}$ ), only one  
13 time computation of Eq. (23) and (24) will suffice. The maximum computation step is 6 times  
14 of Eq. (24) and one time of Eq. (23) when it is in region 1 or 7 and at the same time  $Ri_B$  is large  
15 (i.e.,  $Ri_B > Ri_{Bc6}$ ). Note that the Eq. (24) has only a maximum of 8 elements and a minimum of  
16 4 elements so the calculation is still efficient. **The new equations involve a large number of**  
17 **parameters which increase the complexity of coding. However, the effort of coding the new**  
18 **scheme is minimal as compared to its potential gain, which includes the accuracy of the new**  
19 **scheme and the avoidance of iterations. Besides, a compromise can be made between accuracy**  
20 **and complexity. For models that are not interested in high  $kB^{-1}$  values, region 1 and 2 (i.e.,**  
21  **$10 \leq z/z_0 \leq 10^5$  and  $-0.607 \leq z_0/z_{0h} \leq 100$ ) have provided reasonable coverage (see Garratt,**  
22 **1992; Launiainen, 1995), and the other 6 regions can be ignored. For example, in WRF model**  
23 **MM5 surface module,  $z_{0h} = z_0$  is assumed during the calculation of frictional velocity (Jiménez**  
24 **et al, 2012). While for models that include urban surface effects, it is better to keep all the**  
25 **regions. Further, CB05 probably is not the final solution for the surface flux calculation under**  
26 **stable stratification. The method used to derive non-iterative equations presented here can be**  
27 **used in future studies to transfer the new iterative algorithm to non-iterative equations. Overall,**  
28 **the new equations cover the full range of  $-0.5 \leq kB^{-1} \leq 30$ ,  $10 \leq z/z_0 \leq 10^5$  and stable condition**  
29 **(i.e.,  $0 < Ri_B \leq 2.5$ ), and maintain high accuracy and efficiency. It is expected that its usage in**

1 climate and weather forecast models can lead to better performance in surface flux calculation  
2 under stable conditions, especially over urban surfaces.

### 3 **Acknowledgements**

4 This study is supported by China Meteorological Administration under grant GYHY201006024,  
5 the National Program on Key Basic Research Project of China (973) under grant  
6 2011CB403501, 2012CB417203 and 2010CB428502, the CAS Strategic Priority Research  
7 Program grant XDA05110101, and the National Natural Science Foundation of China under  
8 grant 41275022. The authors would like to acknowledge P. A. Jiménez, J. Dudhia, J. F.  
9 González-Rouco, J. Navarro, J. P. Montávez, E. García-Bustamante, H. Wouters, K. De Ridder  
10 and N. P. M. van Lipzig for their two recent papers which made us aware of the deficiency of  
11 current surface layer flux schemes. We are grateful to two anonymous reviewers for their  
12 careful review and valuable comments, which led to substantial improvement of this manuscript.

13

## 1 **References**

- 2 Beljaars, A. C. M. and Holtslag, A. A. M.: Flux parameterization over land surfaces for  
3 atmospheric models, *J. Appl. Meteorol.*, 30, 327-341, 1991.
- 4 Businger, J. A.: Transfer of momentum and heat in the planetary boundary layer, in *Proceedings*  
5 *of the symposium on the Arctic heat budget and atmospheric circulation*, pp 305-331, 1966.
- 6 Businger, J. A., Wyngaard, J.C., Izumi, Y., and Bardley, E. F.: Flux-profile relationships in the  
7 atmospheric surface layer, *J. Atmos. Sci.*, 28,181-189, 1971.
- 8 Chen, F. and Dudhia, J.: Coupling an advanced land surface–hydrology model with the Penn  
9 State–NCAR MM5 modeling system. Part I: Model implementation and sensitivity, *Mon.*  
10 *Wea. Rev.*,129, 569–585, 2001.
- 11 Cheng, Y.G., and Brutsaert, W.: Flux-profile relationships for wind speed and temperature in  
12 the stable atmospheric boundary layer, *Boundary-Layer Meteorol.*, 114, 519-538, 2005.
- 13 De Bruin, H. A. R., Ronda, R. J., and Van De Wiel, B. J. H.: Approximate solutions for the  
14 Obukhov length and the surface fluxes in terms of bulk Richardson numbers, *Boundary-*  
15 *Layer Meteorol.*, 95, 145-157, 2000.
- 16 **De Ridder K.: Bulk transfer relations for the roughness sublayer, *Boundary-Layer Meteorol.*,**  
17 **134, 257–267, 2010.**
- 18 Dyer, A. J.: The turbulent transport of heat and water vapour in an unstable atmosphere, *Q. J.*  
19 *R. Meteorol. Soc.*, 93, 501-508, 1967.
- 20 Dyer, A. J.: A review of flux-profile relationships, *Boundary-Layer Meteorol.*, 7, 363-372, 1974.
- 21 Fairall, C. W., Bradley, E. F., Rogers, D. P., Edson, J. B., and Young, G. S.: Bulk  
22 parameterization of air-sea fluxes for TOGACOARE, *J. Geophys. Res.*, 101,3747-3764,  
23 1996.
- 24 **Fairall, C. W., Bradley, E. F., Hare, J. E., Grachev, A. A., and Edson. J. B.: Bulk parameterization**  
25 **of air-sea fluxes: updates and verification for the COARE algorithm, *J. Clim.*, 16, 571–591,**  
26 **2003.**
- 27 Garratt, J. R.: *The atmospheric boundary layer*. Cambridge University Press, Cambridge, 1992.
- 28 **Grachev, A. A. and Fairall, C. W.: Dependence of the Monin–Obukhov stability parameter on**  
29 **the bulk Richardson number over the ocean, *J. Appl. Meteor.*, 36, 406–414, 1997.**

- 1 Grachev A.A., Andreas E.L, Fairall C.W., Guest P.S., and Persson P.O.G.: SHEBAflux-profile  
2 relationships in the stable atmospheric boundary layer, *Boundary-Layer Meteorol.*, 124,  
3 315–333, 2007.
- 4 Grachev A. A., Andreas E. L, Fairall C. W., Guest P. S., and Persson P. O. G.: The critical  
5 Richardson number and limits of applicability of local similarity theory in the stable  
6 boundary layer, *Boundary-Layer Meteorol.*, 147, 51-82, 2013.
- 7 Guo, X. and Zhang, H.: A performance comparison between nonlinear similarity functions in  
8 bulk parameterization for very stable conditions, *Environ. Fluid. Mech.*, 7, 239-257, 2007.
- 9 Högström, U.: Review of some basic characteristics of the atmospheric surface layer,  
10 *Boundary-Layer Meteorol.*, 78, 215-246, 1996.
- 11 Holtslag, A. A. M. and de Bruin, H. A. R.: Applied modelling of the nighttime surface energy  
12 balance over land, *J. Appl. Meteorol.*, 22, 689-704, 1988.
- 13 Janjić, Z. I.: The step-mountain eta coordinate model: further developments of the convection,  
14 viscous sublayer and turbulence closure schemes, *Mon. Wea. Rev.*, 122, 927-945, 1994.
- 15 Janjić, Z. I.: The surface layer in the NCEP Eta Model. Eleventh conference on numerical  
16 weather prediction, Norfolk, VA, 19-23 August 1996. Amer. Meteor. Soc., Boston, MA,  
17 pp 354-355, 1996.
- 18 Jiménez, P. A., Dudhia, J., González-Rouco, J. F., Navarro, J., Montávez, J. P., and García-  
19 Bustamante, E.: A revised scheme for the WRF surface layer formulation, *Mon. Wea. Rev.*  
20 140, 898-918, 2012.
- 21 Launiainen, J.: Derivation of the relationship between the Obukhov stability parameter and the  
22 bulk Richardson number for flux-profile studies, *Boundary-Layer Meteorol.* 76, 165-179,  
23 1995.
- 24 Li, Y., Gao, Z., Lenschow, D. H., and Chen, F.: An improved approach for parameterizing  
25 surface-layer turbulent transfer coefficients in numerical models, *Boundary-Layer*  
26 *Meteorol.*, 137, 153-165, 2010.
- 27 Louis, J. F.: A parametric model of vertical eddy fluxes in the atmosphere, *Boundary-Layer*  
28 *Meteorol.*, 17, 187-202, 1979.
- 29 Monin, A. S. and Obukhov, A. M.: Dimensionless characteristics of turbulence in the surface  
30 layer of the atmosphere, *Trudy. Geofiz. Inst. Akad. Nauk. SSSR*, 24, 163-187, 1954.

- 1 Nakanishi, M. and Niino, H.: An improved Mellor-Yamada Level-3 model: Its Numerical  
2 Stability and Application to a Regional Prediction of Advection Fog, *Boundary-Layer*  
3 *Meteorol.*, 119, 397-407, 2006.
- 4 Paulson, C. A.: The mathematical representation of wind speed and temperature in the unstable  
5 atmospheric surface layer, *J. Appl. Meteor.*, 9, 857-861, 1970.
- 6 Poulos, G. S., Blumen, W., Fritts, D. C., Lundquist, J. K., Sun, J., Burns, S. P., Nappo, C., Banta,  
7 R., Newsom, R., Cuxart, J., Terradellas, E., Balsley, B., and Jensen, M.: CASES-99: A  
8 Comprehensive Investigation of the Stable Nocturnal Boundary Layer, *Bull. Amer.*  
9 *Meteorol. Soc.*, 83, 555–581, 2002.
- 10 Sanz Rodrigo, J. and Anderson, P.S.: Investigation of the stable atmospheric boundary layer at  
11 Halley Antarctica, *Boundary-Layer Meteorol.*, 148, 517-539, 2013.
- 12 Sarkar, A. and De Ridder, K.: The urban heat island intensity of Paris: a case study based on a  
13 simple urban surface parametrization, *Boundary-Layer Meteorol.*, 138, 511–520, 2010.
- 14 Sharan, M. and Kumar, P.: Estimation of upper bounds for the applicability of non-linear  
15 similarity functions for non-dimensional wind and temperature profiles in the surface layer  
16 in very stable conditions, *Proc. R. Soc. A.*, 467, 473–494, 2011.
- 17 Skamarock, W. C., Klemp, J. B., Dudhia, J., Gill, D. O., Barker, D. M., Wang W. and Powers,  
18 J. G.: A description of the advanced research WRF version 3, NCAR Technical Note, 2008.
- 19 Song, Y.: An improvement of the Louis scheme for the surface layer in an atmospheric  
20 modelling system, *Boundary-Layer Meteorol.*, 88, 239-254, 1998.
- 21 Sorbjan, Z.: Gradient-based scales and similarity laws in the stable boundary layer, *Quart. J.*  
22 *Roy. Meteorol. Soc.*, 136, 1243–1254, 2010.
- 23 Sorbjan, Z. and Grachev, A.A.: An evaluation of the flux-gradient relationship in the stable  
24 boundary layer, *Boundary-Layer Meteorol.*, 135, 385–405, 2010.
- 25 Sugawara, H. and Narita, K.: Roughness length for heat over an urban canopy, *Theor. Appl.*  
26 *Climatol.*, 95, 291-299, 2009.
- 27 Wouters, H., De Ridder, K. and van Lipzig, N. P. M.: Comprehensive Parametrization of  
28 Surface-Layer Transfer Coefficients for Use in Atmospheric Numerical Models,  
29 *Boundary-Layer Meteorol.*, 145, 539-550, 2012.

- 1 Wyngaard, J. C. and Coté O. R.: Cospectral similarity in the atmospheric surface layer, Quart.
- 2 J. Roy. Meteorol. Soc., 98, 590–603, 1972.
- 3 Yang, K., Tamai, N. and Koike, T.: Analytical solution of surface layer similarity equations, J.
- 4 Appl. Meteorol., 40, 1647-1653, 2001.
- 5



1 Table 1. The 8 regions divided by  $z/z_0$  and  $z_0/z_{0h}$  values.

Region	$z/z_0$	$z_0/z_{0h}$
1	10~160	0.607~100
2	160~ $10^5$	0.607~100
3	10~80	100~ $10^7$
4	80~ $10^5$	100~ $10^7$
5	10~40	$10^7$ ~ $10^{11}$
6	40~ $10^5$	$10^7$ ~ $10^{11}$
7	10~40	$10^{11}$ ~ $1.07 \times 10^{13}$
8	40~ $10^5$	$10^{11}$ ~ $1.07 \times 10^{13}$

2

1 Table 2. The coefficients of Eq. (24).

Region		C <sub>00</sub>	C <sub>10</sub>	C <sub>20</sub>	C <sub>01</sub>	C <sub>11</sub>	C <sub>21</sub>	C <sub>02</sub>	C <sub>12</sub>
1	<i>Ri</i> <sub>Bc1</sub>	0.3095	-0.2852	0.07955	0.03388	-0.01605	0	0	-1.079E-4
	<i>Ri</i> <sub>Bc2</sub>	0.3219	-0.2613	0.06753	0.04838	-0.03101	0.003908	-0.00178	0.001165
	<i>Ri</i> <sub>Bc3</sub>	0.3545	-0.2569	0.06609	0.05837	-0.03934	0.005643	-0.003381	0.002194
	<i>Ri</i> <sub>Bc4</sub>	0.439	-0.3133	0.08619	0.0893	-0.07112	0.01403	-0.005965	0.003806
	<i>Ri</i> <sub>Bc5</sub>	0.6887	-0.5375	0.1616	0.1754	-0.1564	0.03489	-0.01277	0.008101
	<i>Ri</i> <sub>Bc6</sub>	1.706	-1.62	0.5231	0.5124	-0.5026	0.1239	-0.03577	0.02238
2	<i>Ri</i> <sub>Bc1</sub>	0	0.08606	-0.03048	0.09019	-0.07682	0.01693	0	0
	<i>Ri</i> <sub>Bc2</sub>	0.2002	0	-0.01589	0	0.00367	0	0.005057	-0.002399
	<i>Ri</i> <sub>Bc3</sub>	0.4499	0	-0.02397	0.0388	-0.01145	0	0	0
3	<i>Ri</i> <sub>Bc1</sub>	0.3063	-0.2849	0.07886	0.03104	-0.01423	-5.632E-4	3.684E-6	-2.926E-6
	<i>Ri</i> <sub>Bc2</sub>	0.3555	-0.3002	0.07855	0.02617	-0.004769	-0.004012	-1.298E-5	9.907E-6
	<i>Ri</i> <sub>Bc3</sub>	0.5064	-0.4282	0.1229	0.02138	0	-0.00441	0	0
	<i>Ri</i> <sub>Bc4</sub>	1.638	-1.743	0.5813	0.04471	-0.01874	0	0	0
4	<i>Ri</i> <sub>Bc1</sub>	0.09742	0	-0.01096	0.04544	-0.03299	0.006383	0	0
	<i>Ri</i> <sub>Bc2</sub>	0.1768	0	-0.01434	0.03558	-0.02059	0.003327	0	0
	<i>Ri</i> <sub>Bc3</sub>	0.3636	0	-0.0224	0.04607	-0.02506	0.004152	0	0
5	<i>Ri</i> <sub>Bc1</sub>	0	0	0	0.04825	-0.01677	-0.004762	-5.212E-4	2.768E-4
	<i>Ri</i> <sub>Bc2</sub>	0	0	0.08807	0.05219	-0.01822	-0.01245	-8.5E-4	7.516E-4
	<i>Ri</i> <sub>Bc3</sub>	0	0	0.1219	0.0583	-0.02373	-0.01224	-0.001081	9.539E-4
	<i>Ri</i> <sub>Bc4</sub>	0	0	0.1609	0.07789	-0.04617	-0.00736	-0.001399	0.001238
	<i>Ri</i> <sub>Bc5</sub>	0.4437	0	0	0.1349	-0.1388	0.03347	-0.00119	0.001095
6	<i>Ri</i> <sub>Bc1</sub>	0	0	0	0.05594	-0.03245	0.005037	-3.654E-4	1.135E-4
	<i>Ri</i> <sub>Bc2</sub>	0.1945	0	0	0.03347	-0.02116	0.002301	0	8.92E-5
	<i>Ri</i> <sub>Bc3</sub>	0.4288	-0.1436	0.01635	0.03207	-0.01382	0.001571	1.326E-5	-6.424E-6
7	<i>Ri</i> <sub>Bc1</sub>	0	0	0	0.03681	-0.007664	-0.005619	-1.211E-4	0
	<i>Ri</i> <sub>Bc2</sub>	0	0	0	0.03655	0	-0.009977	-2.691E-4	1.057E-4
	<i>Ri</i> <sub>Bc3</sub>	0	0	0	0.03822	0	-0.01036	-3.658E-4	1.769E-4
	<i>Ri</i> <sub>Bc4</sub>	0	0	0	0.0384	0	-0.009243	-3.629E-4	1.471E-4
	<i>Ri</i> <sub>Bc5</sub>	0	0	0	0.05616	-0.02275	0	-5.172E-4	2.261E-4
	<i>Ri</i> <sub>Bc6</sub>	0	0	0	0.1472	-0.1144	0.02796	-0.001218	5.835E-4
8	<i>Ri</i> <sub>Bc1</sub>	0	0	0	0.05139	-0.02991	0.004664	-2.135E-4	6.535E-5
	<i>Ri</i> <sub>Bc2</sub>	0	0	0	0.04919	-0.0197	0.002011	-3.325E-4	7.974E-5
	<i>Ri</i> <sub>Bc3</sub>	0.5775	-0.2236	0.03477	0.03805	-0.01617	0.00177	-2.191E-5	1.067E-5

2

1 Table 3. The coefficients of Eq. (23) for Region1.

2

	Region 1						
	Section 1	Section 2	Section 3	Section 4	Section 5	Section 6	Section 7
C <sub>000</sub>	-1.134	0	0	0	0	0	0
C <sub>100</sub>	31.1	86.35	-280.4	0	0	-17.32	-6.343
C <sub>200</sub>	-71.16	0	3235	0	0	8.773	7.66
C <sub>300</sub>	227.4	0	-6165	0	0	0	-0.7661
C <sub>001</sub>	-0.2094	-11.53	-10.64	0	0	0	0.0125
C <sub>101</sub>	3.293	194.9	193.8	0	1.113	0	-2.203
C <sub>201</sub>	-20.11	-975.4	-1194	-12.37	-97.56	0	0.8896
C <sub>301</sub>	14.42	1472	2161	0	159.4	0	-0.1273
C <sub>002</sub>	0.1476	-2.535	-4.603	0	0	1.919	-0.00827
C <sub>102</sub>	-0.07325	28.24	52.02	11.99	16.33	0	0.3327
C <sub>202</sub>	0.5627	-61.13	-110.7	-15.63	-25.67	0.2679	-0.04613
C <sub>003</sub>	-0.01178	-0.2378	-0.5367	-0.3157	-0.6447	-0.2892	0
C <sub>103</sub>	0.0218	0.7405	1.503	0.2948	0.9718	0	-0.04968
C <sub>010</sub>	1.405	13.6	30.26	0	6.821	10.27	7.513
C <sub>110</sub>	-32.47	-316.2	-314.9	0	-57.13	0	0
C <sub>210</sub>	46.59	1067	186	-108.1	227.3	0	-4.799
C <sub>310</sub>	-38.25	-1494	0	317.8	-244	0	0.5598
C <sub>011</sub>	-0.2286	8.023	9.038	0	0.9287	-3.457	-1.612
C <sub>111</sub>	-1.097	-91.31	-87.06	-12.52	-17.88	-1.617	0
C <sub>211</sub>	-0.3394	213.7	198.6	0	34.41	0	0
C <sub>012</sub>	0	1.035	1.529	0	0.319	-0.07536	0.4666
C <sub>112</sub>	0	-5.072	-7.439	-1.025	-2.452	0	0.0605
C <sub>013</sub>	0	0.03622	0.07369	0.04669	0.08583	0.05146	-0.01808
C <sub>020</sub>	0	-4.699	-10.71	-1.896	-2.195	-3.108	0
C <sub>120</sub>	10.71	97.46	122.1	28.39	22.21	7.948	2.442
C <sub>220</sub>	0	-152.4	-76.91	-14.19	-31.44	-2.985	0.1584
C <sub>021</sub>	0	-1.704	-2.035	0	-0.1355	0.8751	0
C <sub>121</sub>	0	9.069	8.248	2.214	1.976	0.3139	-0.04377
C <sub>022</sub>	0	-0.09576	-0.1263	-0.01472	-0.04636	-0.05131	-0.0694
C <sub>030</sub>	-0.007485	0.4446	1.015	0.3069	0.1708	0.2598	-0.1675
C <sub>130</sub>	-0.9671	-7.991	-10.96	-3.635	-1.623	-0.8513	-0.2181
C <sub>031</sub>	0.003402	0.1138	0.1426	-0.008769	0	-0.05427	0.05052

3

4

1 Table 4. Similar to Table 3, but for Region2.

2

	Region 2			
	Section 1	Section 2	Section 3	Section 4
C <sub>000</sub>	0	0	0	0
C <sub>100</sub>	0	0	41.53	0
C <sub>200</sub>	0	0	0	0
C <sub>300</sub>	0	0	0	0
C <sub>001</sub>	0	0	-1.616	-2.57
C <sub>101</sub>	0	-12.35	0	-2.91
C <sub>201</sub>	0	0	0	0
C <sub>301</sub>	0	0	0	0
C <sub>002</sub>	0	0	0	0.874
C <sub>102</sub>	0	0.5183	0	0.3377
C <sub>202</sub>	0	0	0	0
C <sub>003</sub>	0	0	0	-0.002092
C <sub>103</sub>	0	0	0	-0.01343
C <sub>010</sub>	0.9996	0.8247	0	7.453
C <sub>110</sub>	0	0	15.82	5.4
C <sub>210</sub>	56.57	112.5	-27.37	-1.623
C <sub>310</sub>	0	0	0	0.1999
C <sub>011</sub>	-0.1456	-0.09054	0	0
C <sub>111</sub>	0	0	0	0.4753
C <sub>211</sub>	-12.1	-2.249	0	0
C <sub>012</sub>	0	0.01653	0	-0.2047
C <sub>112</sub>	0.1303	0	0.02288	-0.02581
C <sub>013</sub>	0	0	0	0
C <sub>020</sub>	0	0	0.1062	-0.9043
C <sub>120</sub>	0.295	0.8326	-0.9992	-0.3386
C <sub>220</sub>	0	-9.554	1.56	0.04556
C <sub>021</sub>	0.005508	0	0	0.04682
C <sub>121</sub>	-0.0359	0.07022	0	-0.01924
C <sub>022</sub>	4.067E-4	-0.001333	0	0.01217
C <sub>030</sub>	0	0	0	0.03944
C <sub>130</sub>	0	0	0	0.006516
C <sub>031</sub>	0	0	0	-0.003571

3

1 Table 5. Similar to Table 3, but for Region 3.

2

	Region 3				
	Section 1	Section 2	Section 3	Section 4	Section 5
C <sub>000</sub>	2.001	0	-68.85	-1.514	0
C <sub>100</sub>	-0.7876	0	756.9	0	0
C <sub>200</sub>	0	0	-1100	0	0
C <sub>300</sub>	60.42	368.9	0	19.63	0
C <sub>001</sub>	-0.1401	3.514	0	0.559	0
C <sub>101</sub>	-0.1085	-8.524	-30.13	0	0
C <sub>201</sub>	-2.065	-18.05	86.99	0	0
C <sub>301</sub>	-2.98	-4.852	5.71	-2.424	0
C <sub>002</sub>	0.01334	0.08174	0.7274	-0.002248	0
C <sub>102</sub>	0.0213	0.5791	-2.554	0	0
C <sub>202</sub>	0.1963	0.1207	-0.2169	0.1259	0
C <sub>003</sub>	-3.704E-4	-0.007021	0.01587	8.267E-4	2.413E-4
C <sub>103</sub>	-0.002957	0	0.003912	-0.004141	7.107E-5
C <sub>010</sub>	-1.442	1.207	76.25	-8.751	0
C <sub>110</sub>	1.047	-31.68	-874.1	51.96	1.905
C <sub>210</sub>	0	32.78	1636	-76.51	-1.761
C <sub>310</sub>	0	-25.65	-1040	27.69	0.3658
C <sub>011</sub>	0	-2.096	4.942	-1.349	-0.05227
C <sub>111</sub>	0	2.222	-17.32	1.297	0
C <sub>211</sub>	-1.121	0.3871	14.97	-0.09621	0
C <sub>012</sub>	0	-0.004486	-0.09096	0	0
C <sub>112</sub>	0.0273	-0.06669	0.2281	0	0
C <sub>013</sub>	0	0.001086	-0.002971	2.192E-4	0
C <sub>020</sub>	0.6868	-0.07632	-21.66	3.734	2.165
C <sub>120</sub>	0	14.32	232.4	-6.438	0.6139
C <sub>220</sub>	3.82	2.353	-224.1	6.284	-0.1166
C <sub>021</sub>	-0.01898	0.3396	-1.724	0.2422	-0.07307
C <sub>121</sub>	-0.1228	-0.3281	3.144	-0.2272	0.005656
C <sub>022</sub>	2.845E-4	-3.6E-4	-4.477E-4	0	0
C <sub>030</sub>	-0.06543	0	1.875	-0.4111	-0.3134
C <sub>130</sub>	0.1469	-1.505	-18.02	0.2556	0
C <sub>031</sub>	0.00179	-0.01529	0.1523	-0.009961	0.008105

3

1 Table 6. Similar to Table 3, but for Region 4.

2

	Region 4			
	Section 1	Section 2	Section 3	Section 4
C <sub>000</sub>	0	-3.528	0	0
C <sub>100</sub>	0	0	0	0
C <sub>200</sub>	0	0	0	-8.306
C <sub>300</sub>	0	0	0	1.212
C <sub>001</sub>	0	-0.2511	-1.018	0
C <sub>101</sub>	0	0	0	0
C <sub>201</sub>	-6.267	-10.06	0	0
C <sub>301</sub>	0	0	0	0
C <sub>002</sub>	0	0	0	0
C <sub>102</sub>	0.09808	0.1809	0	0.0279
C <sub>202</sub>	0	0	0	0
C <sub>003</sub>	0	0	6.74E-5	6.853E-4
C <sub>103</sub>	0	0	0.001341	-9.314E-4
C <sub>010</sub>	0.5961	1.375	-2.404	5.253
C <sub>110</sub>	0	2.951	41.12	7.626
C <sub>210</sub>	18.49	68.09	-48.05	-0.2889
C <sub>310</sub>	34.53	0	24.94	0.06073
C <sub>011</sub>	-0.0845	0	-0.06671	-0.3959
C <sub>111</sub>	-0.5106	-1.361	0	-0.07098
C <sub>211</sub>	-0.3543	0	-0.1319	0.003821
C <sub>012</sub>	0.004555	0.003711	0.006818	0
C <sub>112</sub>	0	0	0	0
C <sub>013</sub>	-9.402E-5	0	-1.788E-4	0
C <sub>020</sub>	0.05628	-0.02359	0.5172	-0.5006
C <sub>120</sub>	0.8075	0.305	-4.023	-0.7376
C <sub>220</sub>	0	-3.765	2.074	0
C <sub>021</sub>	0	-0.001535	0	0.04853
C <sub>121</sub>	0.01631	0.07098	0	0.002956
C <sub>022</sub>	-3.8E-5	-2.577E-4	0	0
C <sub>030</sub>	-0.00189	0	-0.0192	0.01968
C <sub>130</sub>	-0.03755	0	0.125	0.025
C <sub>031</sub>	5.177E-5	0	0	-0.001897

3

1 Table 7. Similar to Table 3, but for Region 5.

2

	Region 5					
	Section 1	Section 2	Section 3	Section 4	Section 5	Section 6
C <sub>000</sub>	0	0	-207.7	-587.1	0	0
C <sub>100</sub>	0	77.11	880	2726	7.886	0
C <sub>200</sub>	-2.541	-201.2	-1550	-3759	-0.5889	0
C <sub>300</sub>	25.22	386.1	2201	1605	0	0
C <sub>001</sub>	-0.03201	-0.6831	0	-9.376	-0.4057	0
C <sub>101</sub>	0.1159	0	11.61	-4.513	0	0
C <sub>201</sub>	-0.5745	-7.571	-96.51	70.55	-0.5218	0
C <sub>301</sub>	-0.8502	-8.978	0	-58.16	0	0
C <sub>002</sub>	0.00208	0.07136	0.5093	0.1711	0.01745	0
C <sub>102</sub>	-0.001668	0	0.8873	-0.9373	-0.01349	0
C <sub>202</sub>	0.03737	0.3442	0.2868	1.132	0.01468	0
C <sub>003</sub>	-1.828E-5	0	-0.001909	-0.006865	0	0
C <sub>103</sub>	-3.967E-4	-0.003421	-0.004313	-0.001126	0	0
C <sub>010</sub>	0.4298	0	189.4	286.9	0	0
C <sub>110</sub>	-0.03339	-31.72	-543.8	-903.7	0	0
C <sub>210</sub>	0.05692	2.558	324	407.6	0	0
C <sub>310</sub>	0	0	-80.25	260.2	0	0.08919
C <sub>011</sub>	-0.0233	0	-5.403	0	0	0
C <sub>111</sub>	0	2.695	14.95	14.82	0.2908	0
C <sub>211</sub>	-0.3158	-2.449	-1.706	-26.07	0.1992	0
C <sub>012</sub>	0	-0.05044	-0.4221	0.01062	-0.003177	0
C <sub>112</sub>	0.007595	0.05465	0.164	0.2099	-0.00933	0
C <sub>013</sub>	0	-6.869E-5	-0.00111	9.863E-4	0	0
C <sub>020</sub>	0	0.3612	-53.83	-44.24	0.7321	2.053
C <sub>120</sub>	0	0	89.42	98.98	2.304	0.2534
C <sub>220</sub>	1.793	18.63	34.6	22.67	-2.456	-0.2585
C <sub>021</sub>	0.00249	0.1236	2.704	-0.01096	-0.09448	-0.0338
C <sub>121</sub>	-0.05666	-0.837	-4.573	-1.67	0.007636	0.004269
C <sub>022</sub>	0	0.008316	0.0718	-0.01056	0.002124	0
C <sub>030</sub>	0	-0.06987	4.95	2.138	0	-0.3116
C <sub>130</sub>	0.129	0.8756	-3.112	-4.604	0	0.1241
C <sub>031</sub>	0	-0.01959	-0.3287	0.054	0	0

3

1 Table 8. Similar to Table 3, but for Region 6.

2

	Region 6			
	Section 1	Section 2	Section 3	Section 4
C <sub>000</sub>	0	0.4383	0	-6.744
C <sub>100</sub>	-7.864	0	-41.74	8.8
C <sub>200</sub>	0	0	177	-13.03
C <sub>300</sub>	0	0	-118.2	2.203
C <sub>001</sub>	-0.02699	0	0	-0.1139
C <sub>101</sub>	0.7414	-4.81	-4.006	-0.06103
C <sub>201</sub>	-1.114	5.094	-0.5102	0.2406
C <sub>301</sub>	0	-1.159	0	-0.04635
C <sub>002</sub>	0	0.04547	0	0.01341
C <sub>102</sub>	0	0	0.0567	-0.002749
C <sub>202</sub>	0	-0.1233	0.1868	5.316E-6
C <sub>003</sub>	0	-5.595E-4	0.002457	-1.434E-4
C <sub>103</sub>	1.281E-4	0.002459	-0.006455	0
C <sub>010</sub>	0.244	0	0	6.511
C <sub>110</sub>	1.743	0	27.45	6.369
C <sub>210</sub>	4.749	44.44	-17.37	-0.175
C <sub>310</sub>	11.28	0	-7.74	0.03419
C <sub>011</sub>	0	0	0	-0.3147
C <sub>111</sub>	-0.3093	0	0	-0.06781
C <sub>211</sub>	-0.2208	-0.6068	0.0117	-2.026E-4
C <sub>012</sub>	0	-0.005459	-0.01576	0.002444
C <sub>112</sub>	0.003674	0	0.02102	2.616E-4
C <sub>013</sub>	0	0	-1.975E-5	-5.149E-6
C <sub>020</sub>	0.04168	0	-0.1563	-0.6219
C <sub>120</sub>	0.4341	0.9983	-2.085	-0.598
C <sub>220</sub>	0.6518	-2.874	0.3443	0.002868
C <sub>021</sub>	-0.00208	-0.00152	0.03278	0.03359
C <sub>121</sub>	0	0.01501	-0.0325	0.003178
C <sub>022</sub>	2.895E-5	3.541E-4	5.167E-4	-1.423E-4
C <sub>030</sub>	0	0.006587	0.008163	0.02407
C <sub>130</sub>	-0.01307	-0.04253	0.0854	0.0188
C <sub>031</sub>	1.425E-5	-3.659E-4	-0.001602	-0.001167

3



1 Table 9. Similar to Table 3, but for Region 7.

2

	Region 7						
	Section 1	Section 2	Section 3	Section 4	Section 5	Section 6	Section 7
C <sub>000</sub>	-1.412	-4.502	-104.2	542.4	178.4	0	0
C <sub>100</sub>	6.658	40.44	136.3	-1845	158.8	0	0
C <sub>200</sub>	-5.68	37.42	233.3	2157	-480.9	0	0
C <sub>300</sub>	11.9	0	0	0	0	0	0
C <sub>001</sub>	0.1285	0.3067	13.8	-3.691	-31.49	0	0
C <sub>101</sub>	-0.111	-5.444	-37.21	3.33	47.56	0	0
C <sub>201</sub>	-0.2095	2.053	10.33	-45.62	-4.153	0	0
C <sub>301</sub>	-0.3181	0	0	0	0	0	0
C <sub>002</sub>	-0.004693	0.05302	-0.1157	0.1434	0.3998	0	0
C <sub>102</sub>	0.004467	0	0.5542	0.4557	-0.8692	0	0
C <sub>202</sub>	0.01324	-0.01586	-0.2568	0.08936	0.2504	0	0
C <sub>003</sub>	6.64E-5	0	0	0	0	0	0
C <sub>103</sub>	-2.023E-4	0	0	0	0	0	0
C <sub>010</sub>	0.7122	1.663	16.56	-263.7	-37.94	0	0
C <sub>110</sub>	-4.599	-28.1	0	677.7	-147.8	20.56	0
C <sub>210</sub>	2.705	-11.02	-114.4	-644.2	144.7	-13.42	0
C <sub>310</sub>	0	0	0	0	0	3.002	0
C <sub>011</sub>	-0.04962	0.1172	-3.238	4.44	9.904	-0.5254	0.06758
C <sub>111</sub>	0.01147	1.979	7.578	-3.037	-7.914	0	0
C <sub>211</sub>	-0.1621	-0.7285	0	10.93	-2.224	0	0.003671
C <sub>012</sub>	0.001459	-0.0293	0	-0.08875	-0.1235	0	0
C <sub>112</sub>	0.003514	0.01334	-0.06568	-0.1436	0.1631	0	-6.967E-4
C <sub>013</sub>	-2.01E-5	0	0	0	0	2.282E-4	0
C <sub>020</sub>	0.003692	-0.4475	0	32.93	0	0	0
C <sub>120</sub>	1.299	5.193	-0.1495	-56.58	23.51	-2.349	0.6983
C <sub>220</sub>	0.6516	5.593	18.12	53.14	-2.645	0.628	-0.1455
C <sub>021</sub>	0	-0.009728	0.167	-0.951	-0.7278	0.2176	0
C <sub>121</sub>	-0.03414	-0.3375	-0.6387	0	-0.1801	0.02067	0
C <sub>022</sub>	2.84E-5	0.00347	0.00428	0.02119	0.008599	-0.005396	-4.282E-4
C <sub>030</sub>	6.293E-4	0	0	0	0	-0.4148	0
C <sub>130</sub>	-0.02559	0	0	0	0	0.02245	0
C <sub>031</sub>	0	0	0	0	0	0.01163	0

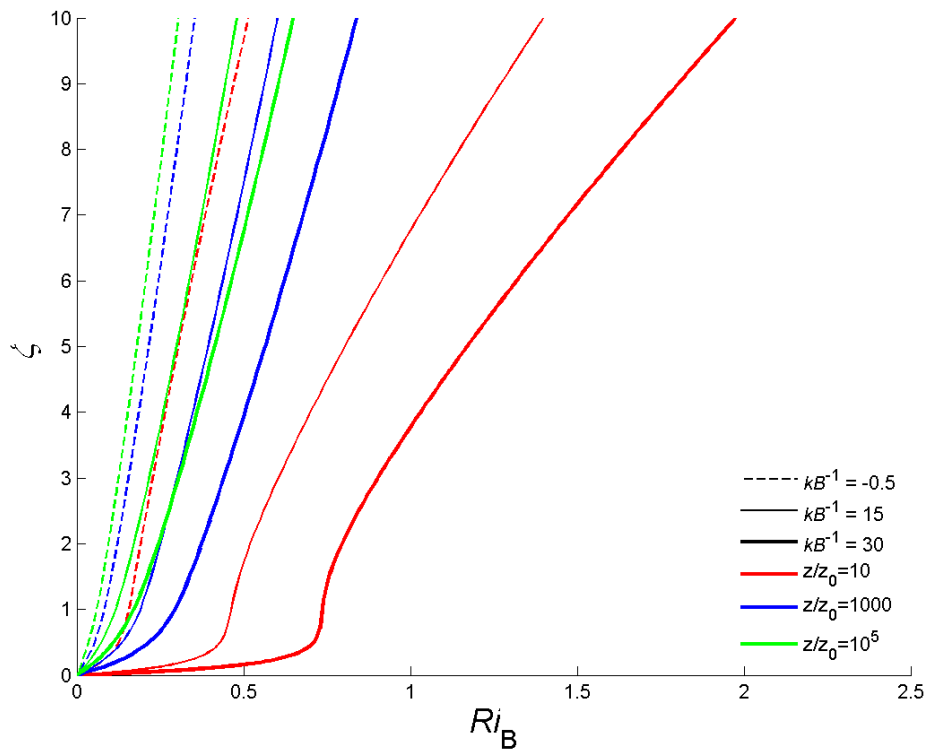
3

1 Table 10. Similar to Table 3, but for Region 8.

2

	Region 8			
	Section 1	Section 2	Section 3	Section 4
C <sub>000</sub>	-3.13	-49.55	0	0
C <sub>100</sub>	5.26	97.14	0	0
C <sub>200</sub>	-29.85	352.5	10.72	0
C <sub>300</sub>	57.04	-573.4	0	0
C <sub>001</sub>	0.2176	2.052	0	0
C <sub>101</sub>	-0.00898	-21.41	0	0
C <sub>201</sub>	-1.756	13.12	0	0
C <sub>301</sub>	-1.663	20.82	-1.354	0
C <sub>002</sub>	-0.007271	0.1357	-0.06227	0
C <sub>102</sub>	0.0304	0.238	0	-0.01477
C <sub>202</sub>	0.05349	-0.7316	0.08799	-0.001292
C <sub>003</sub>	8.978E-5	-0.003367	0.002359	0
C <sub>103</sub>	-6.252E-4	0.006023	-0.002387	3.921E-4
C <sub>010</sub>	0.9846	14.57	-0.2492	0
C <sub>110</sub>	-1.011	0	19.79	0
C <sub>210</sub>	14.45	0	-18.86	-0.8522
C <sub>310</sub>	4.433	-54.39	9.463	0.1065
C <sub>011</sub>	-0.05083	-0.8911	0	0
C <sub>111</sub>	-0.2604	1.478	0	0.374
C <sub>211</sub>	-0.2977	2.13	-0.3291	0.004036
C <sub>012</sub>	0.001361	-9.36E-4	0	0.002528
C <sub>112</sub>	0.00375	-0.04272	0.01369	-0.006853
C <sub>013</sub>	-1.464E-5	1.939E-4	-2.41E-4	-8.747E-5
C <sub>020</sub>	-0.004659	-1.165	0	0
C <sub>120</sub>	0.6393	0	-1.689	-0.4307
C <sub>220</sub>	0	-3.616	1.036	0.01469
C <sub>021</sub>	0	0.06747	0.00194	0.001642
C <sub>121</sub>	0	0.01581	-0.02897	0
C <sub>022</sub>	0	-3.126E-4	8.316E-4	0
C <sub>030</sub>	8.014E-4	0.03485	0.01694	0
C <sub>130</sub>	-0.01934	0	0.06734	0.01348
C <sub>031</sub>	0	-0.001713	-0.001447	0

3

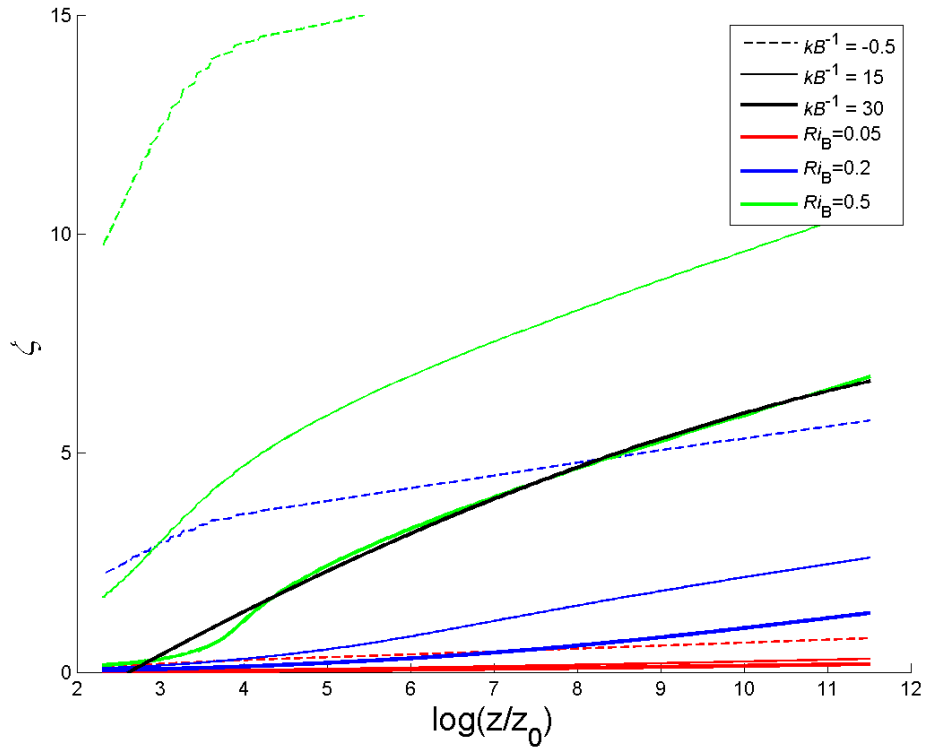


1

2 Figure 1. The relationship between  $Ri_B$  and  $\zeta$  from the precise results of CB05

3

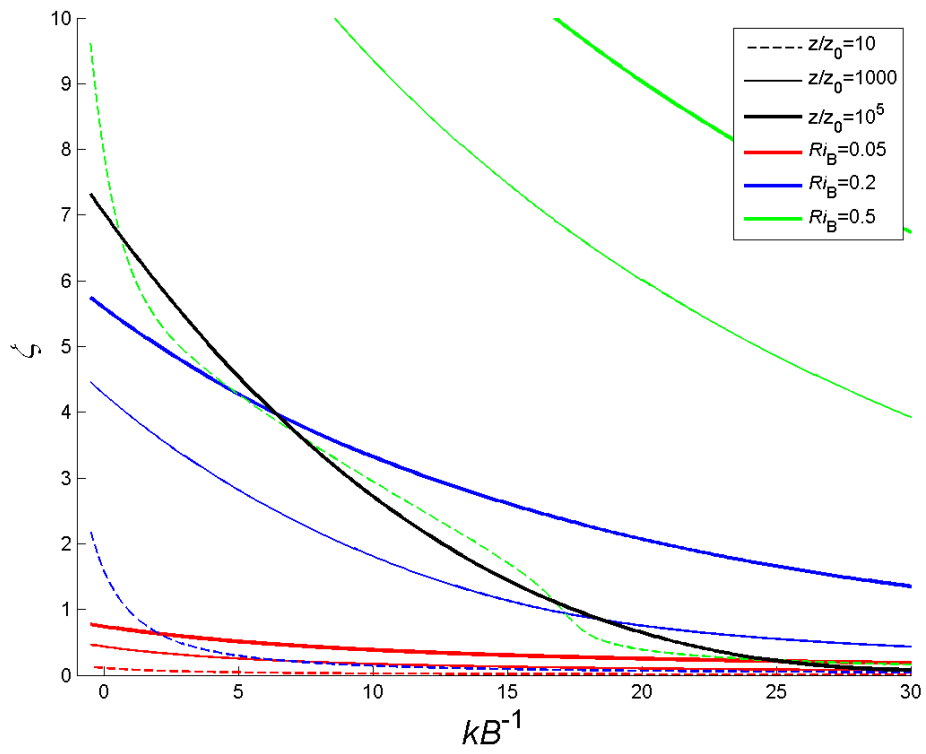
4



1

2 Figure 2. The relationship between  $\log(z/z_0)$  and  $\zeta$  from the precise results of CB05. Black line  
 3 indicates the cubic fit of curve  $k_B^{-1}=30$  and  $Ri_B=0.5$  with least square method.

4

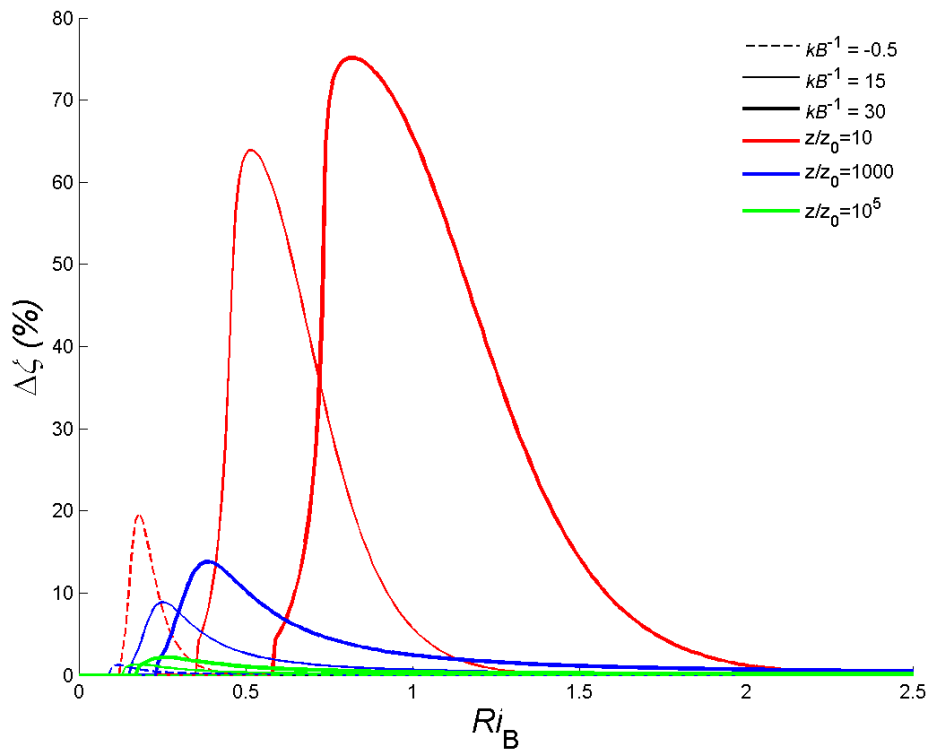


1

2 Figure 3. The relationship between  $\log(z/z_{0h})$  (i.e.,  $kB^{-1}$ ) and  $\zeta$  from the precise results of CB05.

3 Black line indicates the cubic fit of curve  $z/z_0=10$  and  $Ri_B=0.5$  with least square method.

4

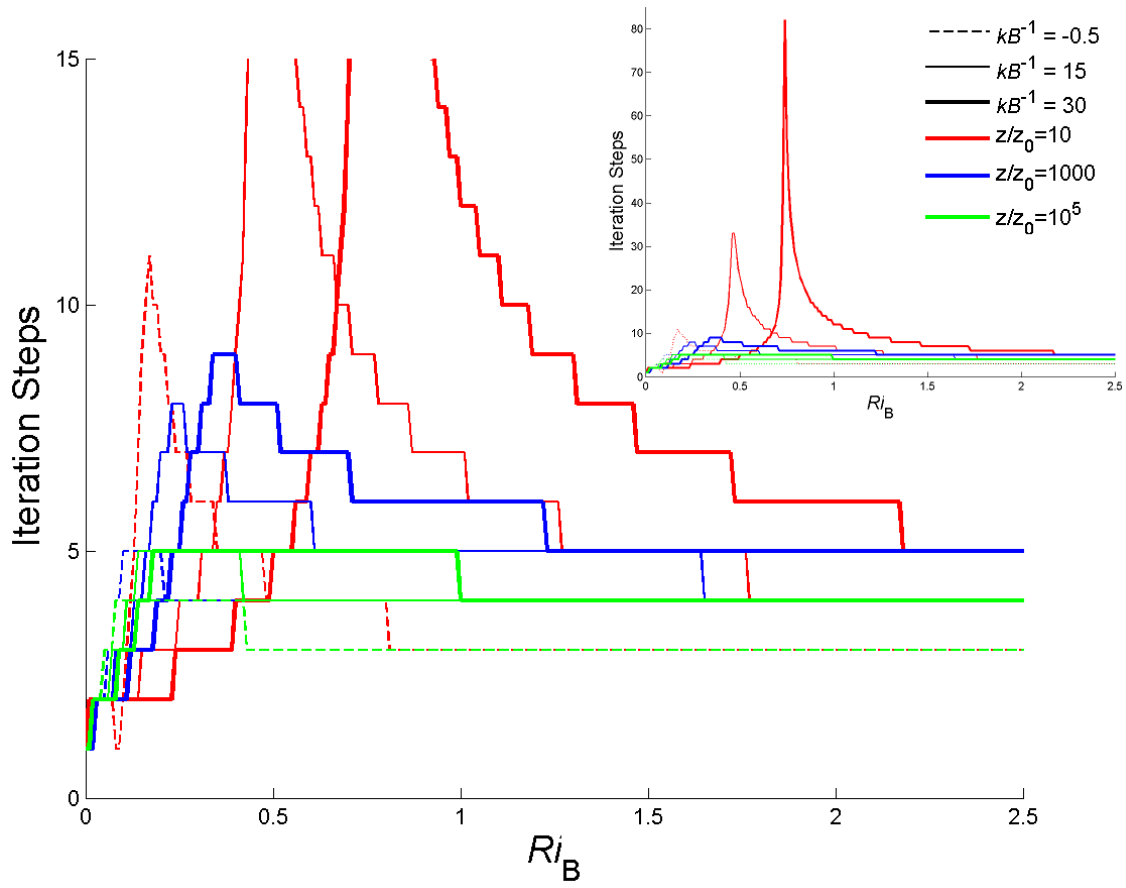


1

2 Figure 4. Relative error after 5 steps of iteration with CB05 equations under certain  $z_0$  and  $z_{0h}$   
 3 conditions.

4

5

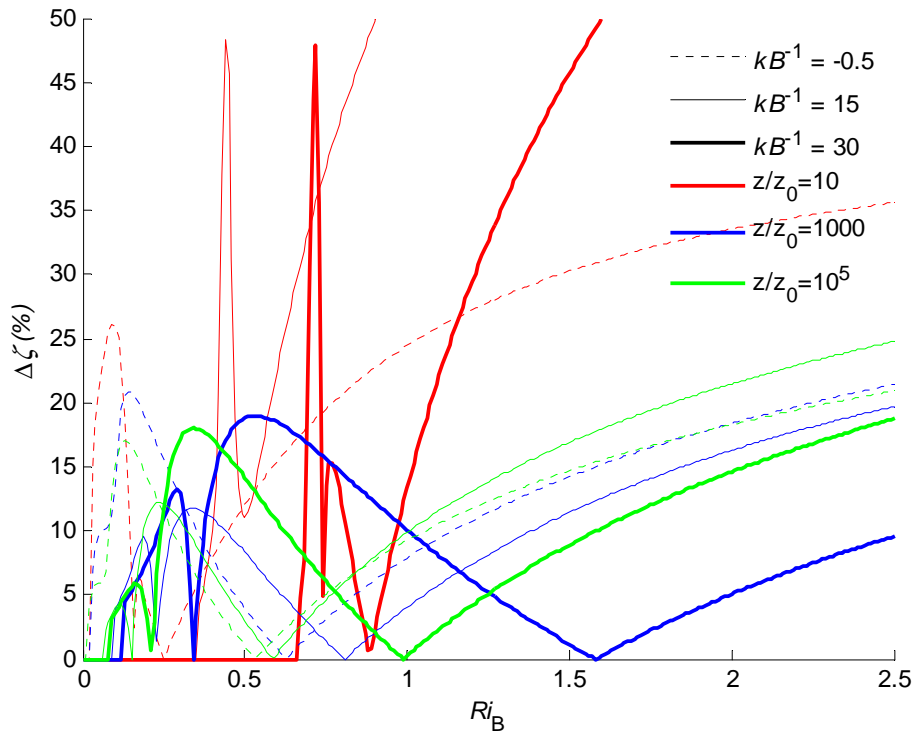


1

2 Figure 5. Steps needed to converge into 5% relative error with CB05 equations under certain  $z_0$   
 3 and  $z_{0h}$  conditions. The inset shows the whole perspective.

4

5

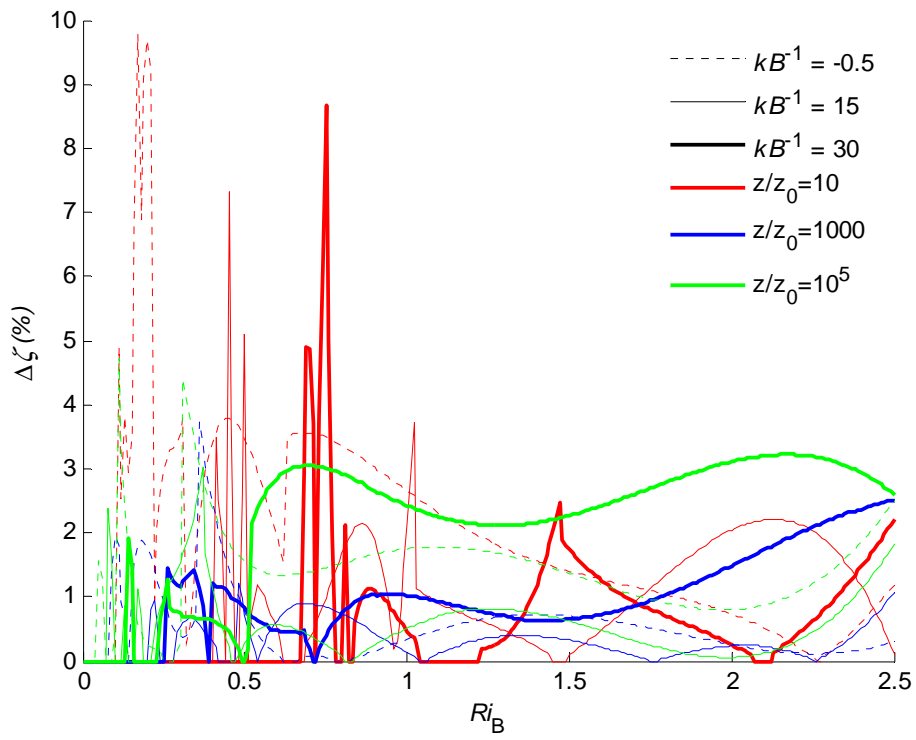


1

2 Figure1. Relative error with WRL12 equations.

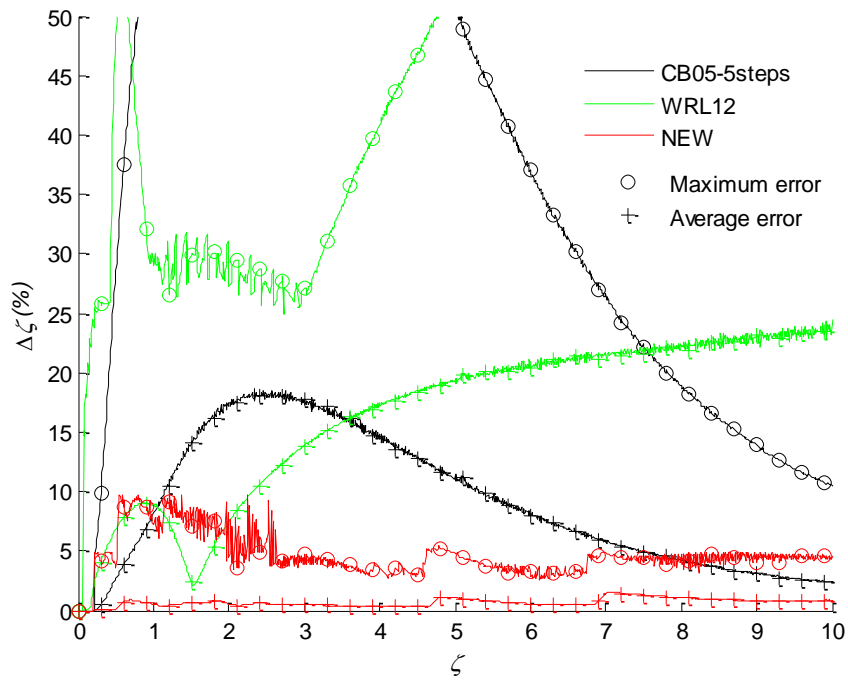
3





1

2 Figure2. Relative error with new equations.

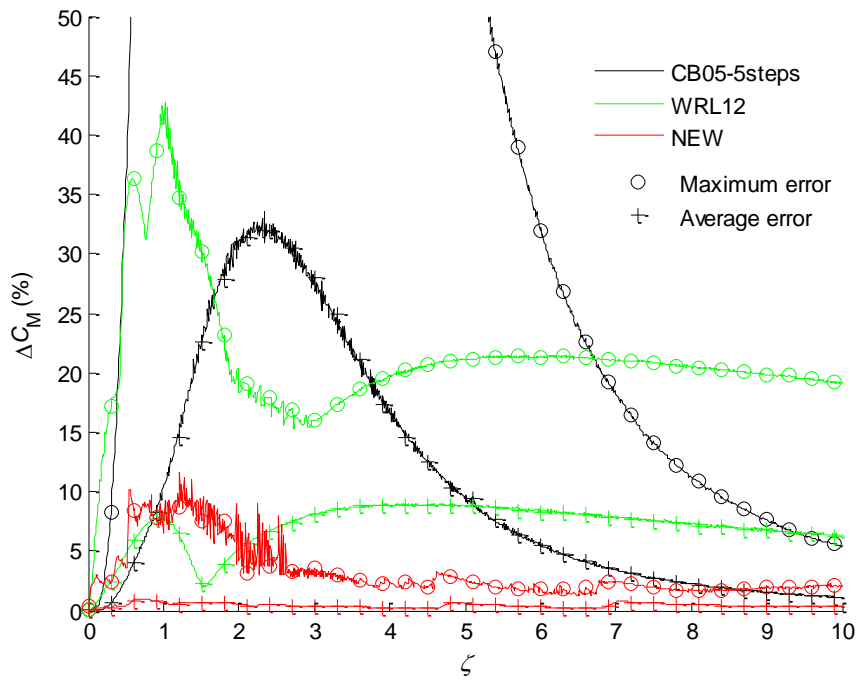


1

2 Figure 8. Maximum (circles) and average (crosses) relative error of  $\zeta$  for CB05 with 5 steps  
 3 iteration (black lines), WRL12 (green lines) and the new scheme (red lines). Errors larger than  
 4 50% are not shown.

5

6

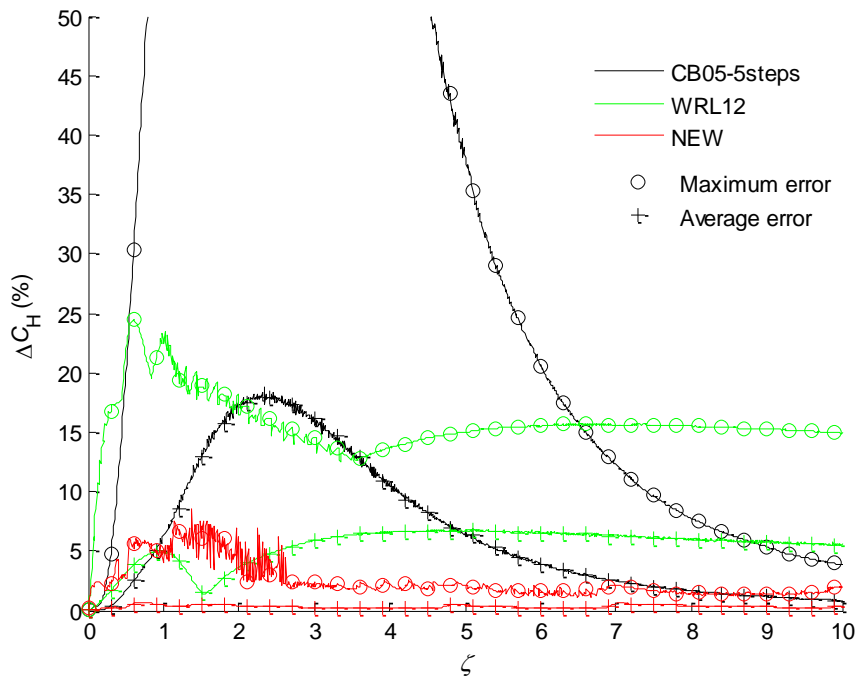


1

2 Figure 9. Similar to Figure 8 but for  $C_M$ .

3

4



1

2 Figure 10. Similar to Figure 8 but for  $C_H$ .

3

4